ISSN 0208-7774 TRIBOLOGIA 3/2017 p. 57–66

Rafał GAWARKIEWICZ*

SEARCH FOR THE MOST USEFUL GEOMETRY OF AN ACOUSTIC JOURNAL BEARING

POSZUKIWANIA NAJKORZYSTNIEJSZEJ GEOMETRII PANWI POPRZECZNEGO ŁOŻYSKA AKUSTYCZNEGO

Key words: air journal bearing, acoustic levitation, ultrasonic levitation, theoretical investigations, experimental validation.

Abstract Computer simulations of a number of journal bearing's geometries utilising acoustic levitation were carried out. The choice of the best geometry depended on the ability of a deformed shape, created by piezo-electric elements, to facilitate squeeze film ultrasonic levitation, and also to create three evenly distributed diverging aerodynamic gaps. Deformations of analysed variants of the bearing's shape were generated by numerical simulations utilising the finite element method. For the chosen shapes of geometry, prototype bearings were made and their usefulness verified experimentally. As a result, the bearing with the highest load carrying capacity was identified.

Słowa kluczowe: poprzeczne łożysko gazowe, lewitacja akustyczna, lewitacja ponaddźwiękowa, badania teoretyczne, weryfikacja doświadczalna.

Streszczenie Przeprowadzono analizę użyteczności szeregu geometrii panwi łożyska poprzecznego wykorzystującego lewitację akustyczną. Wybór najlepszego z przeanalizowanych rozwiązań zależał od zdolności do uzyskiwania kształtu jego powierzchni czynnej sprzyjającego powstaniu ponaddźwiękowej lewitacji akustycznej (wykorzystującej efekt „wyciskania" filmu smarnego), a także umożliwiającego tworzenie zbieżnych równomiernie obwodowo rozmieszczonych szczelin smarnych, które były warunkiem powstawania filmu aerodynamicznego. Kształt części czynnej łożyska zależał od jej deformacji wywoływanej elementami piezoelektrycznymi. Spodziewane deformacje poszczególnych wariantów panwi otrzymywano na drodze symulacji numerycznych wykorzystujących metodę elementów skończonych. Dla wytypowanych geometrii wykonano prototypy łożysk, których przydatność zweryfikowano podczas badań doświadczalnych. Ostatecznie udało się uzyskać postacie panwi łożyskowej o bardzo dużej stabilności pracy, nawet w warunkach impulsowego obciążenia poprzecznego.

INTRODUCTION

High speed aerodynamic bearings often operate in instable ways, because of their low stiffness and the ability to dampen. Hence, it was decided to consider the use of acoustic levitation as an additional possibility to stabilise shaft motion within journal bearings.

The first acoustic levitation phenomena were mentioned in **[L. 1]**. The first detailed theoretical description of standing wave levitation was given in **[L. 2]**, next extended in **[L. 3]**. One of types of acoustic levitation is suspending (light) an object by a standing wave of ultrasonic levitation between radiator and reflector **[L. 4]**. Another type is squeeze film ultrasonic levitation, which happens when surface under levitating object is brought to vibrate with high frequency **[L. 5, 6, 7]**. The first aerodynamic journal bearing using squeeze film pressure was presented in **[L. 8]**. More detailed information about this kind of acoustic bearings can be found, for example, in **[L. 9, 10]**.

It was decided to use second mentioned kind of levitation. It was expected that during the start (but also during the stop), the squeeze film pressure generated

* Gdańsk University of Technology, Department of Machine Design and Vehicles, Faculty of Mechanical Engineering, ul. G. Narutowicza 11/20, 80-233 Gdańsk, Poland, e-mail:gawar@pg.edu.pl.

by oscillating the bearing clearance would lift up the shaft. After it reached sufficiently high rotation speed, the bearing will operate as an aerodynamic bearing due to formation of three converging slots in the bearing's inner surface. To get squeeze film ultrasonic levitation phenomena, it was predicted that high frequency oscillations of the inner bearing's surface caused by piezoelectric transducers (PZT) is required. It was also predicted that forced vibration would be very close to the bearing's resonant frequency, which assures the formulation of three evenly oriented diverging aerodynamic gaps between the shaft and bearing.

ASSUMPTIONS

The main assumptions concerning bearing geometry were active length of 50 mm (in one case 20 mm was accepted) and a nominal inner diameter of 30 mm. Remaining dimensions resulted from predicted manner of bearing fixing in the test rig designed and made at Gdansk University of Technology **[L. 11, 12, 13]**. It was assumed that forces needed for getting the beneficial gap between surfaces of the shaft and of the bearing would be provided by PZT transducers attached to the outer wall of the bearing and spaced 120° along its circumference (according to the applied loading in **Figs. 1** and **3**). It was assumed that it will then be possible to create three narrow converging gaps facilitating the generation of aerodynamic films stabilizing the shaft. It was also assumed that the area of the action of the single PZT element had a width of 5 mm and a length of 15 mm. In some variants, PZT transducers with a square cross-section (5 x 5 mm) and the length of 18 mm were used.

The maximum force generated by the PZT transducers and applied on the defined flat areas was 133.2 N (it corresponded to the voltage of 95 V powering PZT elements). In some versions, an increased number of PZT transducers were considered.

Aluminium alloy was selected for bearing material with the following properties: a Young's modulus of 0.7110^5 MPa, a density of 2.77010^5 kg/m^3, and a Poisson's ratio of 0.33. But some variants of bearings finally were made of steel.

ANALYSED VARIANTS OF BEARING

Analyses of ten variants of the bearing were conducted, which were different in terms of the shape and the number and type of utilised PZT transducers.

W1 version

The first version of the bearing is shown in **Figure 1**. It was assumed that, in this way, the incurred reduction in thickness of the bearing bush would contribute to the creation of equally spaced aerodynamic lubricating slots. **Figure 1b** depicts the way PZT converters apply loads on the bearing.

The simulation results in terms of the total deformation of the whole bearing together with the radial deformation of its inner surface are shown in **Figure 2** .

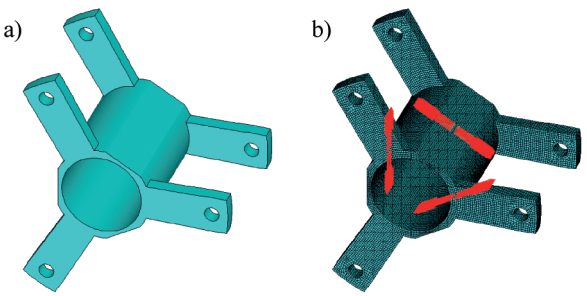

Fig. 1. W1 version of bearing: a) geometry, b) finite elements and PZT loadings

Rys. 1. Wariant W1 panwi łożyskowej: a) geometria, b) podział na elementy skończone oraz sposób przyłożenia obciążeń od elementów PZT

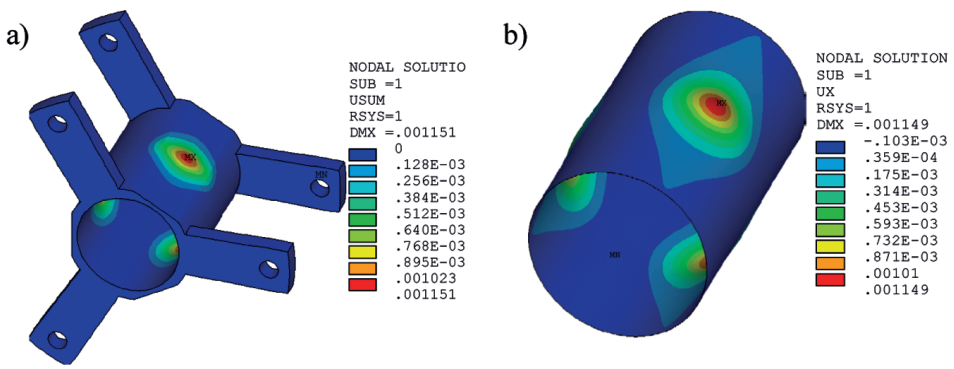

Fig. 2. W1 version of bearing – deformation [mm]: a) total bearing geometry, b) radial of its inner surface (scale about 1950x)

Rys. 2. Wariant W1 – deformacje [mm]: a) całkowite całej panwi, b) promieniowe jej powierzchni wewnętrznej (powiększenie ok. 1950x)

Because of the concern that oscillating dimple, created by PZT transducers, with the depth about 1.1 µm (see **Fig. 2b)** and the very local nature would not provide enough squeeze film effect, it was decided to increase the number of PZT elements to three rows, as shown in **Figure 3**.

The results of the numerical simulation **(Fig. 4)** demonstrated that, in the middle area of the bearing, radial deformation is still about 1.1 µm, but on the edge areas of the bearing, deformation increased twofold to about 2.2 µm. Thus, not only it was not possible to increase the depth and change the region of the dimple, but also conditions of creating aerodynamic film were worsened as well, because of creating lubricant slots on both sides axially divergent to outside of the bearing.

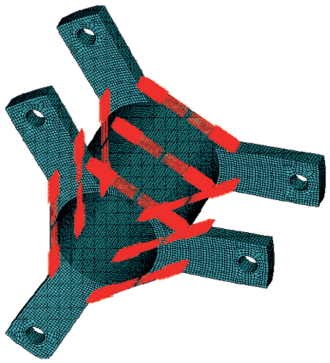

Fig. 3. FEM model of W1 version of bearing witch three rows of PZTs

Rys. 3. Model wariantu W1 panwi łożyskowej z trzema rzędami elementów PZT

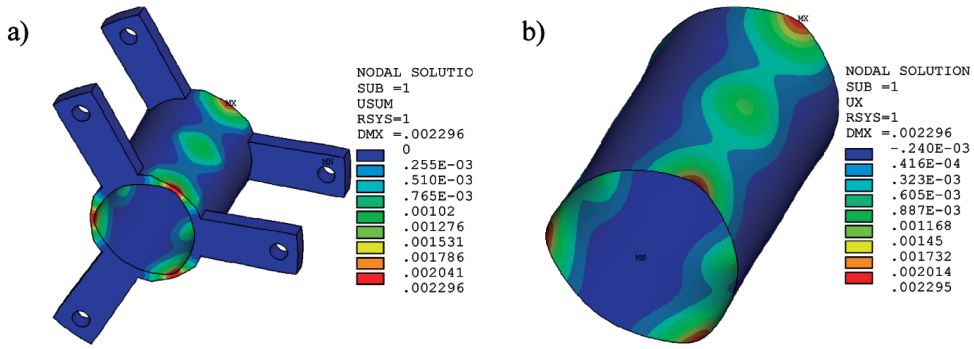

Fig. 4. W1 version of bearing – deformation [mm]: a) total bearing geometry, b) radial of its inner surface (displacements shown in increased scale)

Rys. 4. Wariant W1 – deformacje [mm]: a) całkowite całej panwi, b) jej powierzchni wewnętrznej (przemieszczenia przedstawione w powiększonej skali)

W2 version

In the aim of simplification of the bearing shape and the way of fixing it to the housing, a version of the bearing propped only on three arms located at its centre lengthwise was considered, as shown in **Figure 5**.

Results of the simulation showed the even smaller possibility of obtaining a dimple in the bearing's inner surface, which had a depth below 1 m **(Fig. 5)**. However, its shape, which had an axially converged lubricant gap on both sides, justified making a prototype bearing of this version in the aim of conducting the experimental research.

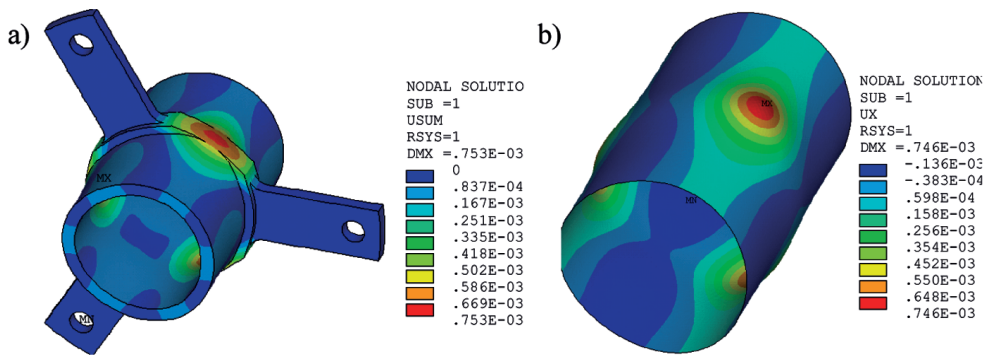

Fig. 5. W2 version of bearing – deformation [mm]: a) total bearing geometry, b) radial of its inner surface (scale about 3300x)

Rys. 5. Wariant W2 – deformacje [mm]: a) całkowite całej panwi, b) jej powierzchni wewnętrznej (powiększenie ok. 3300x)

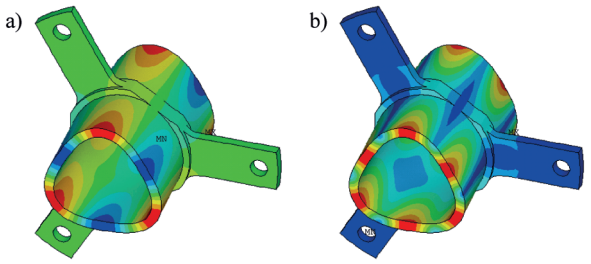

Fig. 6. W2 version of bearing – an example of useful modal shape (at frequency 21.8 kHz): a) total deformation, b) radial deformation

Rys. 6. Wariant W2 – przykład korzystnej postaci drgań własnych panwi (przy częstotliwości 21,8 kHz): a) całkowite deformacje, b) promieniowe deformacje

Experiments were carried out to measure the resistance moment in the bearing when PZT elements were turned off and then when they were powered in an impulse way with the frequency close to resonance. Obtained results confirmed the potential ability to reach a high load carrying capacity of tested version of the bearing **[L. 11, 12]**.

W3 version

In the aim of increasing the convergence of the aerodynamic lubricant gap and getting bigger potential of the squeeze film effect (pumping) caused by oscillating dimples with very high frequency, it was decided to introduce more flexible walls in Variant 3 of the bearing. Therefore, the thickness of the wall was reduced (from 3 up to 2 mm); moreover, the diameter of the ring where PZT transducers were positioned was reduced (from 40 mm to 38.2 mm). Additionally, axial grooves dividing the bearing into three sections from both sides of the bearing were added as shown in **Figure 7**. Grooves, with depth increasing in the outside direction of the bearing, started from flats machined for PZT elements, but they were left without groves.

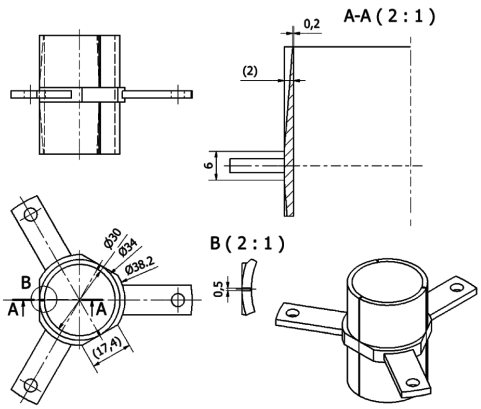

Fig. 7. W3 version of bearing

Rys. 7. Wariant W3 panwi łożyskowej

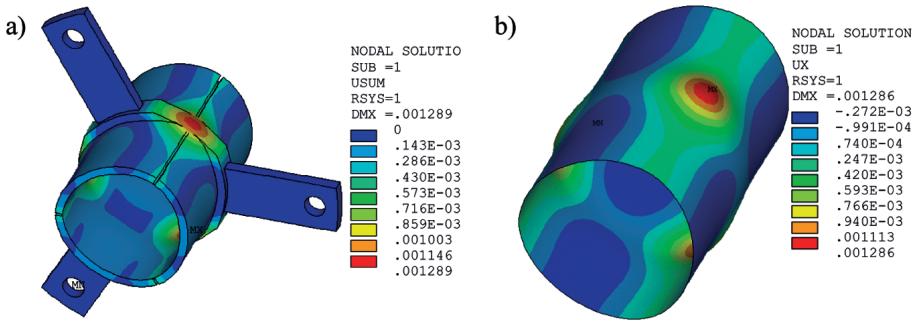

Fig. 8. W3 version of bearing – deformation [mm]: a) total bearing geometry, b) radial of its inner surface (scale about 1950x)

Rys. 8. Wariant W3 – deformacje [mm]: a) całkowite całej panwi, b) jej powierzchni wewnętrznej (powiększenie ok. 1950x)

Results of the numerical simulation demonstrated an improved ability to create dimples in the central region of the bearing's inner surface. The maximum depth of a dimple in this variant could be about 1.3 µm **(Fig. 8)**.

W4 version

In this version, the thickness of the bearing was further reduced from the maximum value of 1 mm in the central region of the bearing to 0.2 mm at its edges **(Fig. 9)**. The diameter of the ring with flats for PZT transducers was also reduced (up to 35 mm).

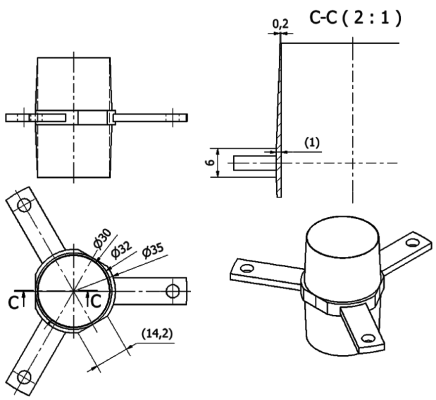

Fig. 9. W4 version of bearing

Rys. 9. Wariant W4 panwi łożyskowej

Results of the numerical simulation showed that the potential for creating dimples on the bearing's inner surface indeed had increased and, according to **Figure 10**, the depth of the dimples was over 3 m. However, because of unfavorable axial profile of lubricant slot diverging to the outside of the bearing, it was decided not to make a prototype bearing of this variant and try to find better one.

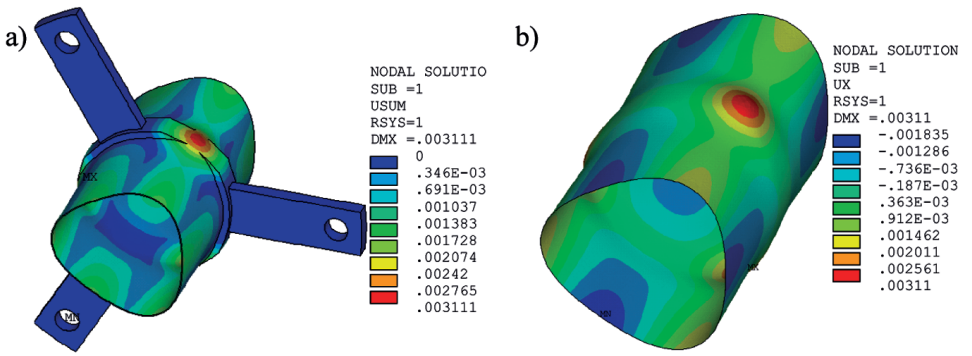

Fig. 10. W4 version of bearing – deformation [mm]: a) total bearing geometry, b) radial of its inner surface (scale about 1950x)

Rys. 10. Wariant W4 – deformacje [mm]: a) całkowite całej panwi, b) jej powierzchni wewnętrznej (powiększenie ok. 1950x)

W5 ersion

In the W5 version, it was decided to make the bearing more flexible. In the centre region (not taking into consideration the central ring for attaching PZT transducers), it had the largest thickness of 0.7 mm, from where the thickness decreased to 0.5 mm. Afterwards, it increased again to 0.7 mm on the length of 7 mm, creating a cone as shown in **Figure 11**. The diameter of the ring for PZT elements was reduced up to 35 mm.

Results from numerical calculations showed that, in the case of W5 version geometry, it was possible to enhance depth of a dimple in the central part of the bearing's inner surface to about 3.5 m (according to **Fig. 12**). It also slightly reduced the axial divergence of the lubricant gap.

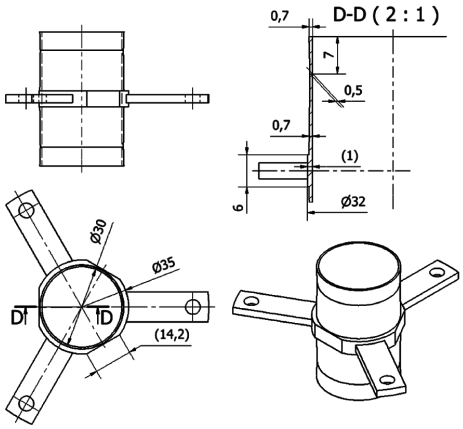

Fig. 11. W5 version of bearing

Rys. 11. Wariant W5 panwi łożyskowej

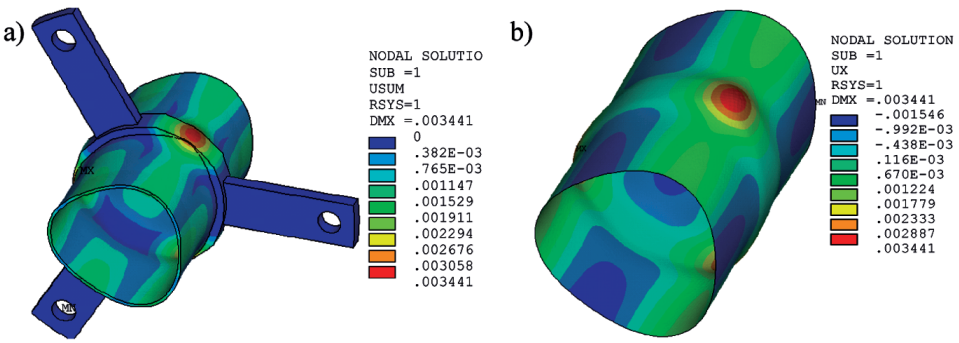

Fig. 12. W5 version of bearing – deformation [mm]: a) total bearing geometry, b) radial of its inner surface (scale about 750x)

Rys. 12. Wariant W5 – deformacje [mm]: a) całkowite całej panwi, b) jej powierzchni wewnętrznej (powiększenie ok. 750x)

W6 version

In the W6 variant – because of technological reasons – the thickness of the bearing shell was increased. In the central part, it had a 2.1 mm thickness, where from (as a cone) the thickness decreased to 0.7 mm, and next it increased again to 1.2 mm, creating a cone with the length of 7 mm **(Fig. 13)**. Additionally, three grooves (symmetrical in the central plane of the bearing) divided the bearing into three sections making the shell more flexible. Grooves **(Fig. 13)** were positioned in planes going through the centres of fixing. The thickness of the bearing below the grooves was constant and equal to 0.4 mm. The diameter of the ring where PZT elements were attached was 36 mm.

Figure 14 shows the results of the computer simulation. It can be seen that this version does not have any advantage over the previous version, because the radial deformation of the bearing's inner surface was smaller – less than 2.5 μm.

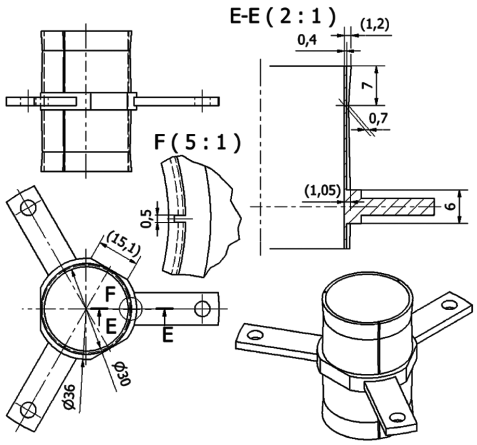

Fig. 13. W6 version of bearing
Rys. 13. Wariant W6 panwi łożyskowej

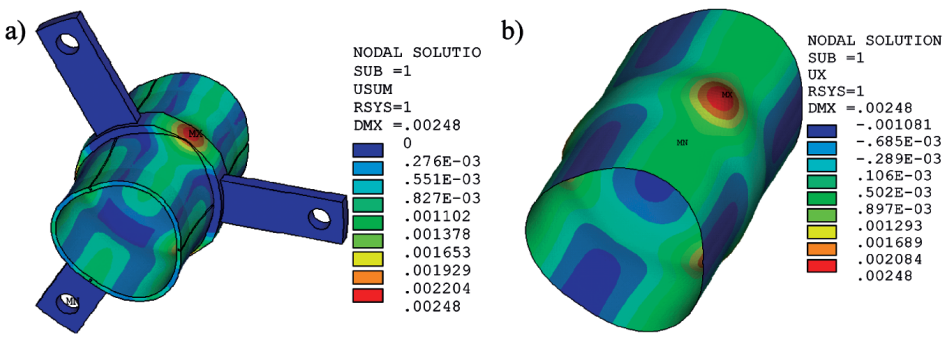

Fig. 14. W6 version of bearing deformation [mm]: a) total bearing geometry, b) radial of its inner surface (scale about 1000x)
Rys. 14. Wariant W6 – deformacje [mm]: a) całkowite całej panwi, b) jej powierzchni wewnętrznej (powiększenie ok. 1000x)

W7 version

Similar to the W6 version, in the central region of this version, the wall thickness was 2.1 mm, from where – as a cone – it decreased to 0.7 mm. As in the previous version, the shell also had a conical shape with a thickness of 1.2 mm on the length of 7 mm on both sides **(Fig. 15)**. Grooves making the bearing more flexible and dividing the shell into three segments were also introduced; however, in this case, they were positioned on the planes symmetrically between the fixing arms.

At the location of grooves, the thickness of the bearing shell was constant and equal to 0.4 mm. The diameter of the ring for PZT elements was 36 mm.

Results of the computer simulation **(Fig. 16)** showed that the ability for the radial deformation in central part of W7 version is similar to that of the previous version and can attain the value of about 2.5 μm. However, the axial profile of the lubricant gap deteriorated, i.e. it became more divergent to the outside direction of the bearing.

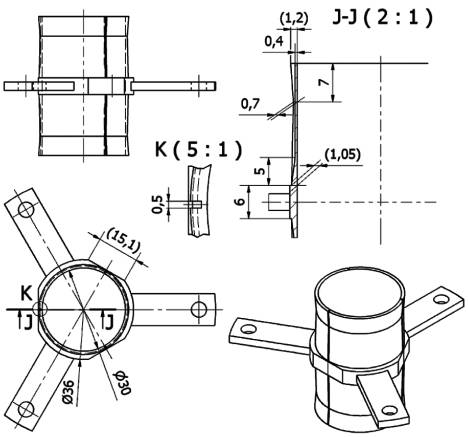

Fig. 15. W7 version of bearing
Rys. 15. Wariant W7 panwi łożyskowej

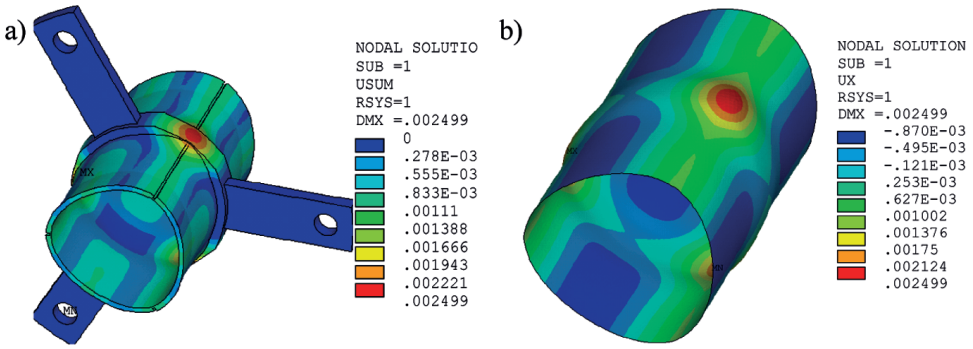

Fig. 16. W7 version of bearing – deformation [mm]: a) total bearing geometry, b) radial of its inner surface (scale about 1000x)

Rys. 16. Wariant W7 – deformacje [mm]: a) całkowite całej panwi, b) jej powierzchni wewnętrznej (powiększenie ok. 1000x)

W8-w version

In the W8-w version, the grooves making a more flexible bearing shell were removed, mainly for technological considerations. The shell had a smaller thickness than in the previous version. In the central part, it had a thickness of 1 mm (from where it decreased as a cone) up to 0.5 mm, where then again it increased up to 1.5 mm, creating a cone with length of 3 mm **(Fig. 17)**. Thickening the rim of the shell, like in previous cases, was aimed at the formation of a closed space between the shaft and bearing. This created an axial lubricant gap converging to the outside direction. The "passage" forming the fixing arms to the shell was made in the gentle technological way, keeping flat areas (about 15.1 mm length) for attaching of PZT transducers.

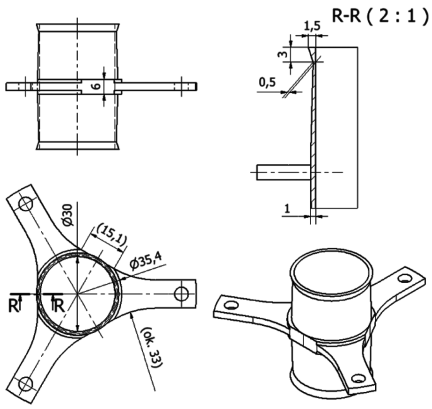

Fig. 17. W8-w9 version of bearing

Rys. 17. Wariant W8-w panwi łożyskowej

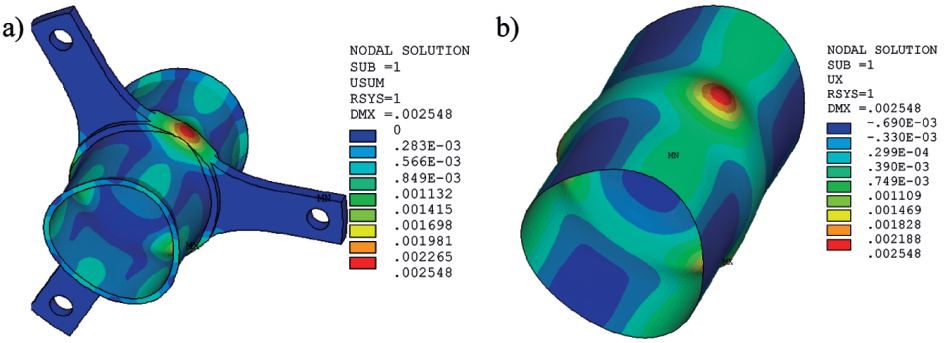

Fig. 18. W8-w version of bearing – deformation [mm]: a) total bearing geometry, b) radial of its inner surface (scale about 1200x)

Rys. 18. Wariant W8-w – deformacje [mm]: a) całkowite całej panwi, b) jej powierzchni wewnętrznej (powiększenie ok. 1200x)

Results from the simulation **(Fig. 18)** demonstrated that the geometry of the W8-w version had a potential for creating dimples in the bearing's inner surface up to about 2.5 µm. Similar results were obtained for some of the previous versions, particularly for the W4 version (see **Fig. 10b**), which enabled creating dimples with depth of 3.1 µm, but the profile of lubricant slots were less favourable. For a better comparison, a computer simulation for Version W8 without curves of passages of fixing arms to bearing shell was carried out. Then it turned out that the potential for radial deformation of W4 and W8 versions is almost the same. The advantage of the W8 version was that it had a more beneficial shape of the deformation of the bearing's inner surface, and in

particular, the outside edges had more wheeled shape, creating a better sealing space between the shaft and bearing.

Additionally, the W8-w version was characterized by a better technological geometry.

Also, modal analysis for this version of the bearing was conducted, and it indicated that resonant frequencies for the beneficial shape of the shell, as expected, were marked out. An example of this beneficial resonant mode of the bearing (for 11.4 kHz) is shown in **Figure 19**.

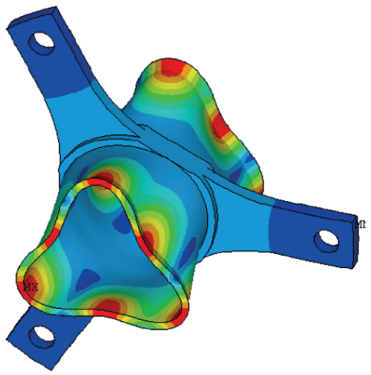

Fig. 19. W8-w version of bearing – an example of useful modal shape (11.4 kHz)

Rys. 19. Wariant W8-w – przykładowa postać drgań własnych panwi (11.4 kHz)

Results generated by theoretical analysis provided support for the decision to make the bearing of this variant. The experimental research was conducted. Obtained experimental results confirmed that, for most frequencies marked out by computer simulation, the load capacity of the bearing was indeed at its highest **[L. 11, 12]**.

W9-w version

At this stage of the research, an attempt was made to find the geometry of the bearing which could assure radial deformation on a larger area than that found for previous variants. Moreover, it was considered beneficial to avoid the divergence of the lubricant gap in the axial direction. The geometry of the W9-w version was a first example of this solution, which was based on the outcomes of earlier studies **[L. 8, 9]**. The shape of the bearing is completely different than considered so far. It consists of connected rigid segments with elastic thinnings performing the role of "hinges" (denoted by Z in **Fig. 20**).

Admittedly, as simulation results indicated, the expected maximum radial deformation of the bearing's inner surface **(Fig. 20b)** was not more than 1.2 μm, which – in comparison with earlier versions – was not a very considerable value; however, the observed shape of the deformation – three evenly orientated aerodynamic slots

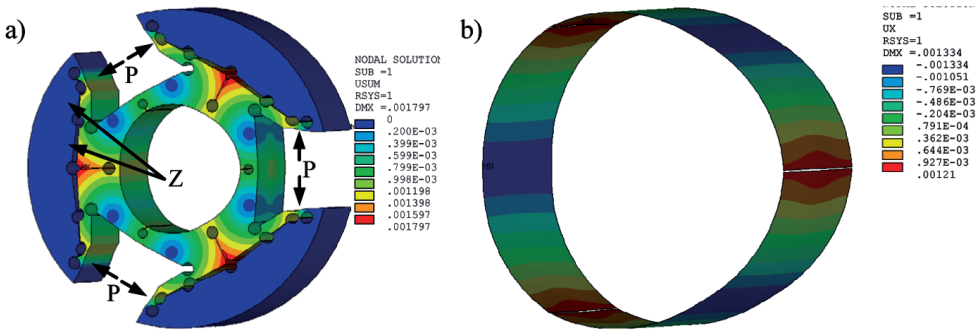

Fig. 20. W9-w version of bearing – deformation [mm]: a) total bearing geometry: P – location of PZT, Z – elastic "hinge"; b) radial of its inner surface (scale about 500x)

Rys. 20. Wariant W9-w – deformacje [mm]: a) całkowite całej panwi: P – miejsce dla elementu PZT, Z – elastyczny „zawias"; b) jej powierzchni wewnętrznej (powiększenie ok. 500x)

gently closing on both sides – was considerably more advantageous than that observed in earlier versions.

Conducted modal analysis provided information on the frequencies of beneficial bearing shapes at which load carrying capacity was at the highest. An example of such beneficial resonant modes of the bearing (for 7.3 and about 27 kHz) is shown in **Figure 21**.

A bearing of this geometry finally was made of steel, and rod-type PZTs were employed and positioned as shown in **Figure 20a**. Results from experimental research confirmed the ability of the bearing to support practically significant loads **[L. 11, 12]** at frequencies marked out by computer simulations.

Fig. 21. W9-w version of bearing – examples of a useful modal shape at the frequencies of 7.3 kHz (to the left) and about 27 kHz (to the right)

Rys. 21. Wariant W9-w – przykłady korzystnych postaci drgań własnych panwi o częstotliwości: 7.3 kHz (po lewej) i ok. 27 kHz (po prawej)

W10-2PZT-w version

In order to increase the load carrying capacity of the bearing, as well as to improve its ability of stable operation, the length of the sleeve of the bearing was enlarged from 20 up to 50 mm. Remaining dimensions and details of geometry did not change **(Fig. 22)**. Additionally, the number of PZT elements was redoubled.

Increasing the length of bearing sleeve together with redoubling the number of PZT elements gave the effect of increased radial deformation of the bearing's inner surface to above 1.5 μm **(Fig. 23b)**. Three

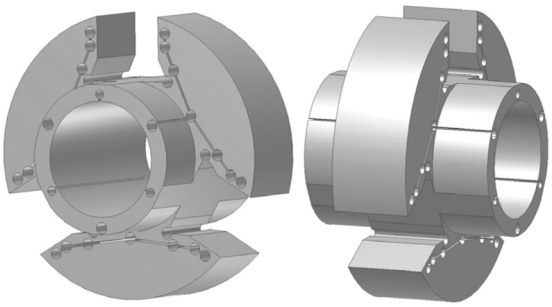

Fig. 22. W10-2PZT version bearing geometry
Rys. 22. Wariant W10-2PZT panwi łożyskowej

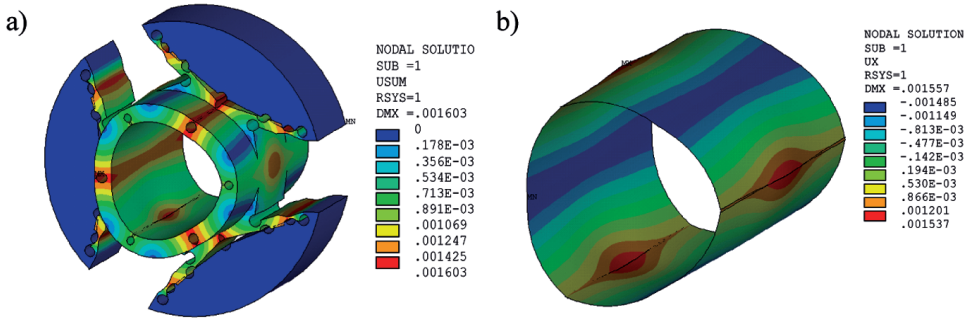

Fig. 23. W10-2PZT-w – the last version of bearing deformation [mm]: a) total bearing geometry, b) radial of its inner surface (scale about 1000x)
Rys. 23. W10-2PZT-w – ostatni wariant łożyska – deformacje [mm]: a) całkowite całej panwi, b) promieniowe powierzchni wewnętrznej (powiększenie ok. 1000x)

aerodynamic slots retained their beneficial deformation in the form of evenly distributed and gently converging gaps on whole length of the bearing.

Conducted modal analysis identified frequencies linked to beneficial deformed shapes of the bearing sleeve. An example of beneficial resonant mode (7.7 kHz) of the bearing is shown in **Figure 24**.

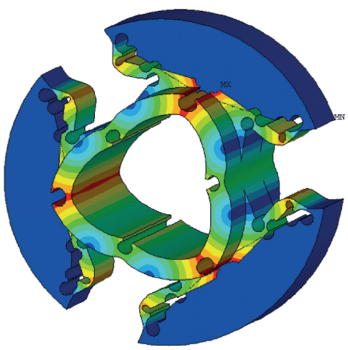

Fig. 24. W10-2PZT-w – last version of bearing – example of mode of vibration (7.7 kHz)
Rys. 24. W10-2PZT-w – ostatni wariant łożyska – przykład postaci drgań własnych (7,7 kHz)

This bearing was also made of steel and underwent experimental testing **[L. 11, 12]**. Experimental results demonstrated that this version is superior to Version W9-w in terms of stable running even under short duration impulse loading **[L. 13]**.

CONCLUSIONS

Conducted numerical simulations for a number of versions of acoustic bearing geometry allowed us to decide on the most beneficial solution in terms of the load carrying capacity **[L. 11, 12]**, and running stability under impulse loading **[L. 13]**. The last of described versions (W10-2PZT-w) had the most beneficial characteristics of operation. However, for technological considerations, a much simpler W8-w version was chosen, even though the experimental research showed its smaller load carrying capacity and stability of operation **[L. 11, 12]**. **Figure 25** presents photographs of bearing of this variant (photograph on the right is showing the bearing fixed in housing for fixing it to the test rig).

Finally, it should be added that the conducted theoretical research on every analysed version of the bearing shorten the time of the search, and it saved costs by eliminating experimental testing of every considered version. Moreover, results from modal analyses shortened the time of the experimental testing providing information on beneficial resonant frequencies and deformation modes of bearings.

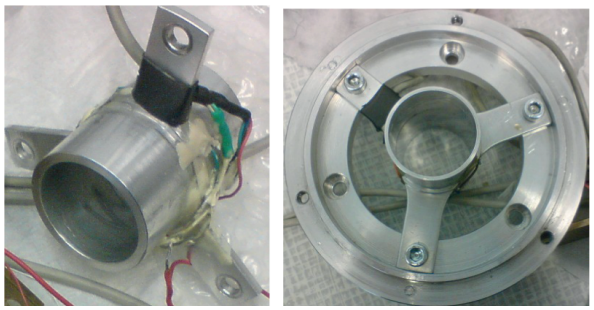

Fig. 25. Constructed W8-w variant bearing solution
Rys. 25. Wykonane łożysko wariantu W8-w

ACKNOWLEDGEMENTS

The author would like to acknowledge the financial support for the research reported in this paper by the scientific project from the National Centre of Science, Poland (Project No. 2012/07/B/ST8/03683).

REFERENCES

1. Poynting J.H., Thomson J.J.: Textbook of Physics, Charles Griffin & Co., 1904.
2. King L.V.: On the acoustic radiation pressure on spheres, Proc. R. Soc., London, 1934.
3. Westervelt P.J.: Acoustic radiation pressure, J. Acoust. Society of America, 29, 26–29, 1957.
4. Vandaele V., Lambert P., Delchambre A.: Non-contact handling in microassembly: Acoustical levitation, Precision Engineering, 29, 491–505, 2005.
5. Stolarski T.A.: Numerical modelling and experimental verification of compressible squeeze film pressure. Tribol. Int. 43(1–2), 356–360, 2010.
6. Atherton M., Mares C., Stolarski T.A.: Some fundamental aspects of self-levitating sliding contact bearings and their practical implementations. Proc. IMechE Part J J. Eng. Tribol. 228(9), 916–927 (2014).
7. Stolarski T.A.: Acoustic levitation – a novel alternative to traditional lubrication of contacting surfaces. Tribol. Jpn. Soc. Tribol. 9(4), 1–7, 2014.
8. Ha D.N., Stolarski T.A., Yoshimoto S.: An aerodynamic bearing with adjustable geometry and self-lifting capacity. Part 1: self-lift capacity by squeeze film. Proc. IMechE Part J J. Eng. Tribol. 219(7), 33–39, 2005.
9. Xue Y., Stolarski T.A., Yoshimoto S.: Air journal bearing utilizing near field acoustic levitation – stationary shaft case, Proc. IMechE, part J, Journal of Engineering Tribology, 225, 120–127, 2011.
10. Stolarski T.A.: Self-lifting contacts – From Physical Fundamentals to Practical Applications, Proc. IMechE, part C: J.Mech. Eng. Sci., 220, 1211–1218, 2006.
11. Stolarski T.A., Gawarkiewicz R., Tesch K.: Acoustic journal bearing – a search for adequate configuration, Tribology International, vol. 92, 387–394, 2015.
12. Stolarski T.A., Gawarkiewicz R., Tesch K.: Acoustic bearing – performance under various load and speed conditions, Tribology International, vol. 102, 297–304, 2016.
13. Stolarski T.A., Gawarkiewicz R., Tesch K.: Extended Duration Running and Impulse Loading Characteristics of an Acoustic Bearing with Enhanced Geometry, Tribology Letters, vol. 65 (2/2017), 2017.